UCRL-TR-202380

LAWRENCE
LIVERMORE
NATIONAL
LABORATORY

INCCA: Integrated Climate and Carbon

Final Report of the LLNL LDRD Strategic Initiative

S. L. Thompson

17 February 2004

This work was performed under the auspices of the U.S. Department of Energy by University of California, Lawrence Livermore National Laboratory under Contract W-7405-Eng-48.

INCCA: Integrated Climate and Carbon
Final Report of the LLNL LDRD Strategic Initiative

S. L. Thompson, Principal Investigator
February 2004

1. The INCCA Strategic Initiative, Rationale and Description

Summary of Rationale

The INCCA (Integrated Climate and Carbon) strategic initiative developed and applied the ability to simulate the fate and climate impact of fossil fuel-derived carbon dioxide (CO_2) on a global scale. Coupled climate and carbon cycle modeling like that of INCCA is required to understand and predict the future environmental impacts of fossil fuel burning. At present, atmospheric CO_2 concentrations are *prescribed*, not simulated, in large climate models. Credible simulations of the entire climate system, however, need to *predict* time-evolving climate forcing using anthropogenic emissions as the fundamental input.

Predicting atmospheric CO_2 concentrations represents a substantial scientific advance because there are large natural sources and sinks of carbon that are likely to change as a result of climate change. Both terrestrial (e.g., vegetation on land) and oceanic components of the carbon cycle are known to be sensitive to climate change. Estimates of the amount of man-made CO_2 that will accumulate in the atmosphere depend on understanding the carbon cycle. For this reason, models that use CO_2 emissions, not prescribed atmospheric concentrations, as fundamental inputs are required to directly address greenhouse-related questions of interest to policymakers.

Overview

The INCCA (Integrated Climate and Carbon) initiative developed the ability to simulate the fate and climate impact of fossil fuel-derived carbon dioxide (CO_2) on a global scale. This capability required interactive, dynamical treatments of both the terrestrial and oceanic ecological and biogeochemical components of the carbon cycle.

A U.S. Carbon Cycle Science Plan (1999) states,

> *"…to predict the behavior of Earth's climate system in the future, we must be able to understand the functioning of the carbon system and predict the evolution of atmospheric CO_2."*

Coupled climate and carbon cycle modeling like that done for INCCA is required to understand and predict the future environmental impacts of fossil fuel burning. At present, atmospheric CO_2 concentrations are *prescribed*, not simulated, in large climate models. To assess impacts of fossil fuel burning, however, we need to *predict* time-evolving atmospheric greenhouse forcing using anthropogenic emissions as the fundamental input. Predicting atmospheric CO_2 concentrations represents a substantial scientific advance because large terrestrial biospheric and oceanic sources/sinks of carbon are key components of the present-day carbon cycle that will likely change in the future. Models driven by prescribed greenhouse gas emission rates (not concentrations) are needed to assess impacts of proposed emission policies.

One of the fundamental scientific research problems of the current age concerns the degree to which human activities may alter global climate (Houghton, et al 1996). The principal source of potential climate change is the radiatively active "greenhouse" gas carbon dioxide (CO_2) produced from burning fossil fuels. There are other man-made and man-influenced greenhouse gases (e.g., methane, nitrous oxide, ozone), but CO_2 has the largest overall effect and is expected to dominate future climate change.

At present, humans introduce about 7 petagrams (or gigatons) of fossil fuel-derived carbon into the atmosphere each year in the form of carbon dioxide. This and previous emissions have resulted in an increase in concentration of atmospheric CO_2 from about 280 parts per million (ppmv) during the mid 19th century to about 370 ppmv today. The atmospheric concentration is expected to continue to increase until it levels off at some "stabilization value" depending on governmental agreements to control emissions.

However, not all anthropogenic CO_2 stays in the atmosphere. Only about half of the emissions accumulate, the so-called "airborne fraction". The rest is taken up by the oceans or vegetation/soils as part of the carbon cycle. These carbon cycle sinks of carbon dioxide are expected to change as climate changes.

The terrestrial (mostly plants) and marine (ocean circulation, chemistry and biology) components of the global carbon cycle transfer large amounts of CO_2 into and out of the atmosphere seasonally and geographically. Thus, the net transfer of carbon that occurs, about half the man-made input, is small compared to the large gross fluxes of the system. This makes simulation a challenge, but more importantly, it helps produce a system that is delicately balanced and sensitive to climate change.

The uptake of carbon dioxide by the oceans occurs primarily in a few regional areas of the high latitudes of the northern and southern hemispheres. These areas are thought to be susceptible to large changes in ocean circulation that could arise from global warming. This concern is based on model simulations and observations from the geologic record of past climate changes.

The long-term uptake of carbon dioxide by land plants can also be perturbed by changes in climate. Recent simulations have shown that interannual variations in rainfall during the past few decades probably resulted in large changes in net carbon uptake by the land biosphere. Even the *sign* of the uptake can vary from year to year. In a globally warmed future, the response of the land biosphere is uncertain, but it has the potential to play a large role in determining how much CO_2 remains in the atmosphere. Added to this is the uncertain direct effect of extra CO_2 on plant growth, the so-called "fertilization" effect.

It is important to emphasize that none of these interactive effects of climate change on the ocean and land components of the carbon cycle is included in today's standard comprehensive climate model projections of future climate. This limitation was addressed in the development of the LLNL INCCA model system.

The key science questions that INCCA addresses are:

- How might the ocean carbon sink change because of future climate change?
- How might the land carbon sink change because of future climate change?

Technical Approach

Our approach relied on the use of existing models that are well developed and published. In only a few instances was it necessary to develop new codes for INCCA, and even then the development relied on a strong foundation of existing work. This approach was possible because we built on previous efforts at LLNL and elsewhere in climate modeling and scientific computing.

Comprehensive and credible modeling of the interactions of the carbon cycle and climate requires models of atmosphere and ocean circulation, the terrestrial (land) carbon cycle, and the ocean carbon cycle. Each of these components is discussed briefly below.

Atmosphere and Ocean Circulation Modeling

We used the emerging *de facto* national standard climate modeling system developed at the National Center for Atmospheric Research (NCAR) in collaboration with other national labs, including LLNL, in association with an extensive university user community. The Community Climate Model Version 3 (CCM3) is used as the atmospheric circulation modeling component in INCCA.

The ocean circulation model we use is a version of the Parallel Ocean Program (POP) developed at the Los Alamos National Laboratory (LANL). A coupled version of POP and CCM3 comprise the model system called PCTM (Parallel Climate Transitional Model) that was developed at NCAR.

Together, the atmospheric and oceanic circulation models (PCTM) are referred to as the climate model portion of INCCA. See Section 2 and 3 of this report for more information.

Ocean Carbon Cycle Modeling

INCCA used the ocean carbon cycle model that has been developed at LLNL by Co-Investigators Ken Caldeira and Jose Milovich. This model performs among the best of those considered by the Ocean Carbon-cycle Model Intercomparison Project, particularly in the Southern Hemisphere. The simulation of anthropogenic carbon dioxide (Caldeira and Duffy, 2000) is among the first to be largely consistent with observations. See Sections 2 and 3 of this report for more information.

Terrestrial Carbon Cycle Modeling

The terrestrial model component of INCCA is IBIS (Integrated Biosphere Simulator) that has been developed by Jonathan Foley and his team at the University of Wisconsin (Foley et al., 1996; Kucharik et al., 2000). IBIS describes the physical, physiological and ecological processes occurring in vegetation and soils in a coherent, mechanistic and simple way.

IBIS reconciles the disparity among previous models by representing the following processes in a single, physically-consistent framework: (a) land surface biophysical processes; (b) ecosystem physiology and carbon balance processes (Foley, 1995); (c) vegetation phenology (e.g., seasonal effects); (d) time-dependent plant growth and competition, and (e) nutrient cycling and soil biogeochemistry.

IBIS has been validated in stand-alone mode with in-situ measurements from very different environments: a tropical forest, a mid-latitude pasture, a boreal forest, a prairie and a soybean crop (Delire and Foley, 1999). Its surface water balance has also been validated over the continental United States (Lenters et al., 2000). The model has also been tested with a wide range of continental- and global-scale data, including measurements of river discharge, net primary production, vegetation structure, root biomass, soil carbon, litter carbon, and soil CO_2 flux (Kucharik et al., 2000). The ability of IBIS to simulate short and long time scale processes and carbon cycling in both vegetation and soils makes IBIS a good tool for use within a coupled climate and carbon cycle modeling system.

The development of IBIS yielded two important landmarks in vegetation modeling:

- IBIS was the first published dynamic global vegetation model that could be used to simulate transient changes in ecosystem processes, vegetation cover, and carbon cycle effects in response to climate and land use change.
- IBIS was the first time-dependent ecosystem model to be incorporated within atmospheric general circulation models. While at NCAR, Thompson, the INCCA PI, worked with Foley to incorporate IBIS into the GENESIS earth system model (Foley et al., 1998, Thompson and Pollard, 1995).

The INCCA Project Team

Principal Investigator

Starley L. Thompson is a member of the Climate and Carbon Cycle Modeling Group of the Atmospheric Science Division of LLNL. Expertise: climate modeling, land surface processes and earth system model development. He led the GENESIS Earth System

Modeling project at the National Center for Atmospheric Research before coming to LLNL in 1999.

Co-Investigators

Ken Caldeira is a member of the Climate and Carbon Cycle Modeling Group of the Atmospheric Science Division. He is an authority on the simulation of the oceanic component of the carbon cycle and was co-director of the DOE Ocean Carbon Sequestration Center. He is a member of the US Carbon Cycle Science Plan Interagency Advisory Committee.

Christine Delire is a Research Associate at the Center for Sustainability and the Global Environment (SAGE) in the Institute for Environmental Studies at the University of Wisconsin. Expertise: climate-vegetation interactions and global climate modeling.

Philip B. Duffy is leader of the Climate and Carbon Cycle Modeling Group of the Atmospheric Science Division. He is a recognized authority on numerical modeling of ocean circulation and on climate change.

Jonathan Foley is an Associate Professor of Atmospheric & Oceanic Sciences and Environmental Studies at the University of Wisconsin, Madison. He is an internationally recognized authority on terrestrial ecosystem and biogeochemical modeling, and a member of the US Carbon Cycle Science Plan Interagency Advisory Committee.

Bala Govindasamy is a member of the Climate and Carbon Cycle Modeling Group of the Atmospheric Science Division. Expertise: climate modeling and use of the NCAR climate models.

Jose Milovich is a computational physicist at the Center for Applied Scientific Computing (CASC). Expertise: fluid dynamics models on various high performance platforms.

Arthur Mirin is a computational physicist at the Center for Applied Scientific Computing (CASC). Expertise: climate models on massively parallel computers.

Technical Outcome

We have developed a climate-carbon simulation capability and have performed multi-century simulations with the fully coupled INCCA system. Sections 2 and 3 of this report describe the results and significance of our primary work.

Section 1, References

A U.S. Carbon Cycle Science Plan, 1999: A report of the Carbon and Climate Working Group, Jorge L. Sarmiento and Steven C. Wofsy, co-Chairs. US Global Change Research Program. Washington, D.C. 69pp.

Bousquet, P., P. Peylin, P. Ciais, C.Quere, P. Friedlingstein, P.P. Tans, 2001: Regional changes in carbon dioxice fluxes of land and ocean since 1980, *Science*, **290**, 1342-1346

Caldeira, K. and P.B. Duffy, 2000: The role of the Southern Ocean in uptake and storage of anthropogenic carbon dioxide, *Science***, 287,** 620-622.

Delire C. and J.A. Foley, Evaluating the Performance of a Land Surface / Ecosystem Model with Biophysical Measurements from Contrasting Environments, *Journal of Geophysical Research, vol 104, D14*, 16895-16909, 1999.

Duffy, P.B., and K. Caldeira, Sensitivity of Simulated Salinity in a Three-dimensional Ocean Model to Upper-Ocean Transport of Salt From Sea-Ice Formation,*Geophys. Res. Lett.* , ***24,*** 1323-1326, 1997.

Foley, J.A., 1995: An equilibrium model of the terrestrial carbon budget. *Tellus* **47B**, 310-319.

Foley, J.A., I.C. Prentice, N. Ramankutty, S. Levis, D. Pollard, S. Stich and A. Haxeltine, 1996: An integrated biosphere model of land surface processes, terrestrial carbon balance, and vegetation dynamics. *Glolal Biogeochemical Cycles*, **10**, 603-628.

Foley, J.A., S. Levis, I.C. Prentice, D. Pollard, and S.L. Thompson, 1998: Coupling models of climate and vegetation**.** *Global Change Biology*, ***4***, 561-579.

Govindasamy, B., K. Caldeira, and P. B.Duffy, 2001: Geoengineering Earth's radiation balance to mitigate climate change from a quadrupling of CO_2 (accepted for publication in *Global and Planetary Change*).

Govindasamy, B., and Caldeira, K., 2000: Geoengineering Earth's radiation balance to mitigate CO_2-induced climate change , *Geophys. Res. Lett*., **27** , No. 14 , p. 2141

Houghton, J.T., L.G. Meira Filho, B.A. Callandar, N. Harris, A. Kattenberg, and M. K. (Eds.), 1996. *Climate Change 1995, The Science of Climate Change*. Intergovernmental Panel on Climate Change, Cambridge University Press, Cambridge (UK).

Kucharik, C.J., J.A. Foley, C. Delire, V.A. Fisher, M.T. Coe, J. D. Lenters, C. Young-Molling, N. Ramankutty, J.M. Norman, and S.T. Gower, Testing the performance of a dynamic Global Ecosystem Model: Water balance, carbon balance, and vegetation structure, *Global Biogeochemical Cycles*, 14(3), pp 795-825, 2000.

Lenters, J.D., M.T. Coe, and J.A. Foley (2000). Surface water balance of the continental United States, 1963-1995: Regional evaluation of a terrestrial biosphere model and the NCEP/NCAR reanalysis. Journal of Geophysical Research (Atmospheres) 105 (D17), 22,393-22,425., 2000.

Thompson, S.L. and Pollard, D., 1995: A global climate model (GENESIS) with a Land-Surface-Transfer Scheme (LSX). Part 1: Present climate simulation. *J. Climate*, **8**, 732--761.

Thompson, S.L and B. Govindasamy, 2000: Interannual variability of the carbon cycle in a coupled model of climate and the terrestrial biosphere. Presented at the American Geophysical Union Annual Meeting, San Francisco, December 2000.

2. Effect of limited CO_2 fertilization on computed future climate: Quantifying uncertainty in the INCCA coupled climate-carbon model

Fossil fuel burning and some land-use changes release CO_2 into the atmosphere, where it traps radiation and warms the planet. The response of the land biosphere to this CO_2 increase and climatic change is not fully understood. Higher CO_2 concentration directly stimulates leaf photosynthesis and ultimately plant growth when water and nutrients are available. Higher CO2 also favors stomatal closure increasing the water-use efficiency of the plants and favoring growth in water-limited situations. Biomass may thus be expected to increase with higher atmospheric CO_2 levels. However, recent experiments indicate that positive effects of CO_2 fertilization may saturate quickly, and higher global temperatures may accelerate respiration leading to biomass loss. To evaluate the approximate upper and lower limits of land sequestration of carbon, we performed two simulations using the fully coupled INCCA carbon-climate ocean-atmosphere general circulation model. In one, the land biosphere continues to be vigorously fertilized by added CO_2 and absorbs CO_2 from the atmosphere throughout the 21st century. In the second case, CO_2 fertilization of the land-biosphere is assumed to saturate in year 2000. In the latter case, the land biosphere becomes a net source of CO_2 to the atmosphere by 2050, and the land sequestration of carbon decreases from 42% to 5% of the total emissions between 1870 and 2100. The predicted atmospheric CO_2 concentration at year 2100 differs by 336 ppmv between the two cases, representing a 40% difference. We conclude that current uncertainties in the competing effects of CO_2-fertilization and increased temperature preclude determination of whether the land biosphere will amplify or damp the direct CO_2 effects of fossil-fuel burning and land-use change.

The physical climatic system and the carbon cycle are a tightly coupled system, as changes in climate affect exchange of atmospheric CO_2 with the land biosphere and the ocean. Changes in these CO_2 fluxes affect Earth's radiative forcing and the physical climatic system. Any changes in the function of either the terrestrial biosphere or the ocean – whether anticipated or not – could have significant effects on the fraction of fossil fuel CO_2 that stays in the atmosphere (1). The magnitude of the feedbacks within the coupled system is poorly constrained. Results from two recent modeling studies (2,3) led to different conclusions regarding the role of the land biosphere in future global change. Both used coupled climate-carbon ocean-atmosphere general circulation models representing the dynamic response of Earth's climate and carbon system to CO_2 emissions. In the HadCM3 simulation (2), the land biosphere becomes a net source of CO_2 to the atmosphere by year 2050, whereas in the IPSL simulation (3), it remains a net sink throughout the 21^{st} century. Here, we show that we can produce this change of sign in biosphere response by changing only one unique assumption in a fully coupled three-dimensional model: whether CO_2-fertilization rapidly saturates in terrestrial ecosystems.

Higher atmospheric CO_2 concentration stimulates leaf-photosynthesis and favors stomatal closure allowing more efficient use of available water (4). Models incorporating this dynamic without nutrient constraints to growth tend to be more sensitive to CO_2 fertilization (5, 6). However, in real ecosystems, availability of nitrogen or phosphorous may limit growth, diminishing the sensitivity to added CO_2 (7-9). In a recent study using results from six land biosphere models, it is shown that the estimated future availability of nitrogen is much less (by a factor of two) than is required to support CO_2 fertilization in six CO_2-only simulations and four CO_2-climate simulations (9). There is also experimental evidence that the net production of some ecosystems may decline after a few years of exposure to elevated CO_2 levels and global changes like increased temperature and precipitation predicted by models (10).

To investigate the dynamics of the land biosphere in the coupled climatic system, we developed the INCCA (INtegrated Climate CArbon) model of the dynamics and carbon-balance of the ocean, atmosphere, and land-surface. The physical ocean-atmosphere model is the NCAR/DOE PCTM model (11, 12), which is a version of the NCAR CCM 3.2 model (13) coupled to the LANL POP ocean model (14, 15). The climate model is coupled to a terrestrial biosphere model, the Integrated Biosphere Simulator version 2 or IBIS2 (16, 17), and an ocean biogeochemistry model. The horizontal resolution of land and atmosphere models is approximately 2.8° in latitude and 2.8° in longitude with 18 vertical levels. The ocean model has a horizontal resolution of (2/3)° with 40 vertical levels.

IBIS2 is a model of land-surface physics, canopy physiology, plant phenology, vegetation dynamics and competition, and carbon cycling for natural vegetation. It simulates surface water, energy, and carbon fluxes on hourly timesteps and integrates them over the year to estimate annual water and carbon balance (16, 17). The annual carbon balance of vegetation is used to predict changes in the leaf area index and biomass for each of 12 plant functional types, which compete for light and water using different ecological strategies. IBIS2 also simulates carbon cycling through litter and soil organic matter.

The ocean biogeochemistry model is based on the Ocean Carbon-cycle Model Intercomparison Project (OCMIP) “biotic” protocol (18). This model predicts air-sea CO_2 fluxes, biogenic export of organic matter and calcium carbonate, and distributions of dissolved inorganic carbon, phosphate, oxygen, alkalinity, and dissolved organic matter. In the OCMIP protocol, export of biogenic materials is computed to maintain observed upper ocean nutrient concentrations. However, because our simulations involve changes in ocean circulation, we cannot make the assumption that surface nutrient concentrations remain stationary. Therefore, we replaced the OCMIP export formulation with a formulation based on that of Maier-Reimer (19, 20)

We integrated the fully coupled model for more than 200 years to equilibrate to an 1870 “pre-industrial” initial condition (21). We perform three model cases starting from this pre-industrial initial state:

(i) "Control” case with no CO_2 emissions and thus no change in radiative forcing for the period 1870-2100. Model drift evaluated for the period 1900-2100 is a cooling of 0.35 K in mean surface temperature, and a 3.14 ppmv increase in atmospheric CO_2 concentration. Both are residuals from a slight imbalance in the initial state. Since the control drifts are minimal, they are not subtracted from the other simulations in our analysis.

(ii) "Fertilization" case with CO_2 emissions specified at historical levels for 1870-2000 (22) and that follow the IPCC scenario SRES A2 from 2000-2100 (1). Non-CO_2 greenhouse gas concentrations are specified at historical levels for 1870-2000 and

SRES A2 levels from 2000-2100 (1). Land use emissions are taken from (23) for the historical period and from the SRES A2 scenario thereafter. There is no change in aerosol forcing. In this scenario, total emissions reach 29 GtC per year in 2100 AD from present day values of 8 GtC per year.

(iii) "Saturation" case is identical to the fertilization case except the CO_2 fertilization is assumed to saturate at the year 2000 concentration (366 ppmv); the land model is forced not with the predicted CO_2 after year 2000, but with a prescribed CO_2 concentration of 366 ppmv.

We believe that these cases will bracket the reasonable range of nitrogen and/or other limitation on carbon sequestration in the terrestrial biosphere. Since IBIS2 is one of the most responsive models to CO_2 fertilization (6), the fertilization case will probably approximate an upper limit to the land uptake of carbon assuming unlimited nitrogen/nutrient availability. Capping all fertilization at its year 2000 value in the saturation case will approximate a strongly nitrogen/nutrient limited system.

Figure 1a shows that assumptions regarding CO_2-saturation of the land biosphere greatly affect the atmospheric concentration of CO_2. Year 2100 atmospheric CO_2 concentrations are 336 ppmv higher in the saturation case than in the fertilization case. In the SRES A2 scenario, 1790 GtC are emitted to the atmosphere over the 21st century; atmospheric CO_2 content increases by 776 (366 ppmv) and 1489 (702 ppmv) GtC in our fertilization and saturation cases, respectively.

The global climate-carbon cycle feedback factor is a useful system metric defined as the ratio of CO_2 change when climate is changing to the CO_2 change when climate is constant (24). We performed a constant-climate simulation with full emissions to determine this factor and obtained a value of 1.13 for our fertilization case. The feedback factors for similar fertilization simulations are 1.19 for IPSL (3) and 1.68 for HadCM3 (2). Therefore, our model shows the weakest positive feedback between climate and the carbon cycle of the current published results for fertilization cases. Note, however, that our feedback factor increases to 2.05 in our saturation case. This is an indication of the uncertainty in quantifying the climate-carbon cycle feedback arising from a single model assumption.

The temperature difference at 2100 between the saturation and fertilization cases is only 0.7 K (Fig. 1b), but it should be noted that the climatic system has large thermal inertia due to the large heat capacity of the oceans. If the simulations were run to equilibrium with the year 2100 CO_2 values, the temperature difference would be approximately 1.1 C (estimated from the PCTM equilibrium climate sensitivity of 2.1 K per doubling of CO_2)

Simulation results (Fig. 2a) show that assumptions regarding the saturation of CO_2-fertilization fluxes can affect the sign of atmosphere/land-biosphere CO_2 flux by century's end. In the case of the land biosphere, there is competition between direct CO_2 effects and temperature effects. As discussed above, direct CO_2 effects can be expected to lead to increased biomass, but temperature effects can lead to increased heterotrophic respiration and loss of soil carbon (2, 3, 6, 25), at least until a possible acclimation of soil microbiology to the higher temperatures. In the "saturation" simulation, by century's end, the land-biosphere has become a net source of CO_2 to the atmosphere, as temperature effects dominate CO_2-fertilization effects. In the "fertilization" simulation, CO_2-

fertilization effects dominate temperature effects, resulting in continued net biosphere growth.

In contrast to the HadCM3 simulation (2), but in agreement with the IPSL simulation (3), our land carbon cycle model does not become a net source of carbon to the atmosphere in the fertilization case. In the fertilization simulation with HadCM3 (2), vegetation carbon begins to decline, and a drying and warming of Amazonia initiates loss of forest and soil carbon. A loss of vegetation biomass does not occur in either of our simulations, but soil carbon does decline by year 2100 in our saturation case.

Between year 2000 and year 2100, ocean/atmosphere carbon fluxes show significant differences between the two simulations (Fig. 2b). Ocean carbon storage increases by 269 and 357 GtC in the two simulations (Fig 2c). Ocean uptake is greater in the "saturation" simulation because atmospheric CO_2 concentrations are greater, driving an increased flux of CO_2 from the atmosphere to the ocean (26, 27). However, surface warming tends to reduce the dissolution of atmospheric CO_2 in the ocean. Surface warming also causes increased thermal stratification, which inhibits downward transport of anthropogenic carbon. However, with increased stratification, the residence time of nutrients in the euphotic zone increases, allowing a greater fraction of nutrients to be exported from the surface layers as particulate organic carbon. This effect tends to counteract some of the direct physical effects of increased stratification (26, 27). The direct CO_2 effects appear to be much larger than the temperature effects; hence CO_2 added to the atmosphere drives an increased flux into the ocean in the saturation case.

Cumulative emissions since 1870 reach 2200 GtC by year 2100 (Fig. 2c). In the fertilization case, the land biosphere and the oceans sequester 919 GtC (42%) and 346 GtC (15.5%) of the total emissions respectively. In the saturation case, the corresponding amounts are 104 GtC (5%) and 435 GtC (19.5%). Therefore, land sequestration of carbon due to the degree of CO_2 fertilization varies from 5% to 42% of the total emissions in our model. The remaining amounts 935 GtC (42.5%) and 1661 GtC (75.5%) stay in the atmosphere in the fertilization and saturation cases respectively.

The C:N of soil in our model is approximately 11. Assuming a constant C:N ratio of 200 for live biomass (9), the total land ecosystem nitrogen increases by 20 Gt between year 2000 and 2100 in the fertilization case. This is much larger than estimates which show that only 6 Gt of additional nitrogen could accumulate in the terrestrial biosphere by 2100 (9). In contrast, in the saturation case nitrogen in the terrestrial biosphere declines by 8 Gt during the same period. A large accumulation of nitrogen in one case and its release in the other suggest that our simulations bracket reasonably the range of nitrogen/nutrient limitations on carbon sequestration in the terrestrial biosphere.

The geography of simulated carbon uptake in the fertilization case over the period 1870-2100 (Fig. 3) shows that anthropogenic carbon is stored on land primarily in areas of high vegetation productivity (Amazonia, central Africa, south and southeast Asia, and the boreal forests). Currents and circulation make storage somewhat more uniform for the ocean, but it is higher in the North Atlantic and Mid-Southern Oceans, which reflects proximity to regions of net CO_2 uptake (28, 29).

Even without the nutrient limitations, the enhanced physiological effects of CO_2 on productivity and water use efficiency could asymptote at high CO_2 concentration (30, 31). If saturation of CO_2-fertilization will occur before saturation of greenhouse-warming IR-absorption bands, the carbon loss due to warming may be the dominant long-term impact on the land-biosphere; the ability of land to sequester future emissions will be hampered. The climate model used here has temperature sensitivity to increased CO_2 (2.1 K per doubling)(1) that is at the lower end of the range of the general model population (1.5 to 4.5 K)(33). A more sensitive climate model would increase the amount of warming, increasing heterotrophic respiratory fluxes even more. Hence, high climate sensitivity is more likely to amplify carbon losses from the land biosphere; a low climate-sensitivity is more likely to damp the climate effects of CO_2 emissions, with carbon uptake by the biosphere dominated by CO_2 fertilization.

We are in the infancy of developing mechanistic understanding of the controls on land-biosphere carbon fluxes and representing that understanding in global gridded models. Right now, whether the land-biosphere damps or amplifies global warming seems to depend on highly uncertain assumptions regarding the response of the biosphere to increased CO_2 and a changed climate. These uncertainties could perhaps be narrowed with investigation of carbon dynamics across a broad range of ecosystems and climatic regimes, often including manipulation experiments, and redoubled efforts to represent those dynamics numerically. Without this research, we cannot predict if the land-biosphere will help or hinder our efforts to stabilize climate.

Section 2, References and Notes

1. Intergovernmental Panel on Climate Change (IPCC), *Climate Change 2001, The Scientific Basis*, Cambridge University Press, New York, USA, 2001.
2. P. M. Cox, R. A. Betts, C. D. Jones, S. A. Spall, and I. J. Totterdell, *Nature*, **408**, 184 (2000).
3. P. Friedlingstein et al., *Geophys. Res. Lett.*, **28**, 1543 (2001).
4. Owensby, C.E., J. M. Ham, A. K. Knapp, L. M. Auen, *Global Change Biology*, **5**, 597 (1999).
5. D. W. Kicklighter et al., *Tellus*, **51B**, 343 (1999).
6. W. Cramer et al., *Global Change Biology*, **7**, 357 (2001).
7. D. S. Schimel, *Nature*, **393**, 208 (1998).
8. K. J. Nadelhoffer et al., *Nature*, **398**, 145-148 (1999).
9. B. A. Hungate, J. S. Dukes, M. R. Shaw, Y. Luo, and C. B. Field, *Science*, **302**, 1512 (2003).
10. M. R. Shaw, E. S. Zavaleta, N. R. Chiarillo, E. E. Cleland, H. A. Mooney, C. B. Field, *Science*, **298**, 1987 (2002).
11. W. M. Washington et al., *Climate Dynamics*, **16**, 755 (2000).
12. G. A Meehl, et al., *J. Climate* (in press)
13. J. T. Kiehl et al., Description of the NCAR Community climate Model (CCM3). *NCAR Tech. Note*. NCAR/TN-420+STR, (1996).
14. J. K. Dukowicz, R. D. Smith, *J. Geophys. Res.*, **99**, 7991 (1994).
15. M. E. Maltrud, R. D. Smith, A. J. Semtner, A. J. Malone, *J. Geophys. Res.*, **103**, 30825 (1998).
16. J. A. Foley et al., *Global Biogeochem. Cycles*, **10**, 603 (1996).
17. C. J. Kucharik et al., *Global Biogeochem. Cycles* **14** (3), 795 (2000).
18. R. G. Najjar, J.C. Orr, Biotic How-To, Revision 1.7, Ocean Carbon-cycle Model Intercomparison Project (OCMIP) (1999), http://www.ipsl.jussieu.fr/OCMIP/phase2/simulations/Biotic/HOWTO-Biotic.html
19. E. Maier-Reimer, *Global Biogeochemical Cycles*, **7(3)**, 645 (1993).
20. Export formulation is taken from (17): $J_{PROD} = (1/\tau) \bullet g(PAR) \bullet Q_{10}^{(\Delta T/10)} \bullet P^2 / (P_{1/2} + P)$, where J_{PROD} is phosphate uptake rate for production of both exported particulate organic matter and dissolved organic matter; τ is the time constant for phosphate removal from the surface layer at 25^0C in the case of sufficient nutrients and light (here taken to be 60 days); light sensitivity of growth, g(PAR), was modeled according to (34); temperature dependence on growth rate was modeled using Q_{10}=2 following (35); P is the phosphate concentration; following (17), we used a half saturation value for phosphate, $P_{1/2}$, of 2e-5 mol/m^3.
21. When IBIS2 was coupled to PCTM, biases in surface temperature and precipitation appeared. Precipitation biases caused vegetation errors that, in turn, amplified precipitation biases in regions where surface-atmosphere moisture recycling is known to be important. This erroneous feedback effect resulted in unacceptable vegetation in some areas, particularly parts of the Amazon. To correct this, a precipitation correction scheme was implemented. At every surface

grid point and every time step the simulated precipitation field is multiplied by a constant that is a function of position, but otherwise static throughout all runs. The constant acts to move the model's simulated present-day annual mean precipitation towards an observed climatology. However, we maintain the model's global conservation of water and energy. The surface temperature bias was removed by reducing the solar constant from by 1.5 % from 1367 Wm^{-2}.

22. G. Marland, T. Boden, R. Andres, Global, regional, and national annual CO2 emissions from fossil-fuel burning, cement production and gas flaring: 1751-1999, *CDIAC NDP-030*, Carbon Dioxide Information Analysis Center, Oak Ridge National Laboratory, Tennessee.
23. R. Houghton, *Tellus*, **55B**, 378 (2003).
24. P. Friedlingstein, J.-L. Dufresne, P. M. Cox, P. Rayner, *Tellus*, **55B**, 692 (2003).
25. F. Joos, et al., *Global Biogeochemical Cycles*, **15**, 891 (2001).
26. J. L. Sarmiento, C. Le Quere, *Science*, **274**, 1346 (1996).
27. J. L. Sarmiento, M. C. Hughes, R. J. Stouffer, S. Manabe, *Nature*, **393**, 245 (1998).
28. M. E. Wickett, K. Caldeira, P. B. Duffy, *J. Geophys. Res. (Oceans)*, **108**, art. no. 3189 (2003).
29. K. Caldeira, P. B. Duffy, *Science*, **287**, 620 (2000).
30. A. W. King, W. M. Post, S. D. Wullschleger, *Climate Change*, **35**, 199 (1997).
31. M. Cao, F. I. Woodward, *Nature*, **393**, 249 (1998).
32. D. R. Chantal, *Geophys. Res. Lett.*, **30**, 1983 (2003).
33. Intergovernmental Panel on Climate Change (IPCC), *Climate Change The IPCC scientific assessment*, Cambridge University Press, New York, USA, 1990.
34. R. C. Tian et al., *Deep-Sea Research*, **47**, 637 (2000).
35. D. Wolf-Gladrow, U. Riebesell, *Mar. Chem.*, **59**, 17 (1997).

Section 2, Figures

Figure 1. (a) Simulated atmospheric CO_2 from 1870 to 2100. Unforced control (black), fertilization case (green), and saturated case (red). Black dots are observed CO_2 concentrations. If CO_2 fertilization saturates early, the land-biosphere becomes a net source of CO_2 to the atmosphere, amplifying anthropogenic CO_2 emissions. (b) Simulated global mean surface temperature for the same cases as (a).

Figure 2. (a) Global flux of carbon from land to atmosphere. Unforced control (black), fertilization case (green), and saturated case (red). In the saturated case the land becomes a net source of carbon by year 2050. (b) The same as (a) but for carbon flux from ocean to atmosphere. (c) Global carbon change from the 1870 "pre-industrial" starting point. Total earth system (black), land (solid), and ocean (dashed). Fertilization case (green), and saturated case (red)

Figure 3. The simulated geography of carbon stored in the earth system over the period from 1870 to 2100 (column integrated carbon in kg C / m^2) in the fertilization case. Anthropogenic carbon is stored primarily in areas of high vegetation productivity and/or cooler climates over land. Owing to currents, storage is somewhat more uniform for the oceans, but higher in the North Atlantic and Mid-Southern oceans which reflects proximity to regions of net CO_2 uptake.

Section 2, Figure 1

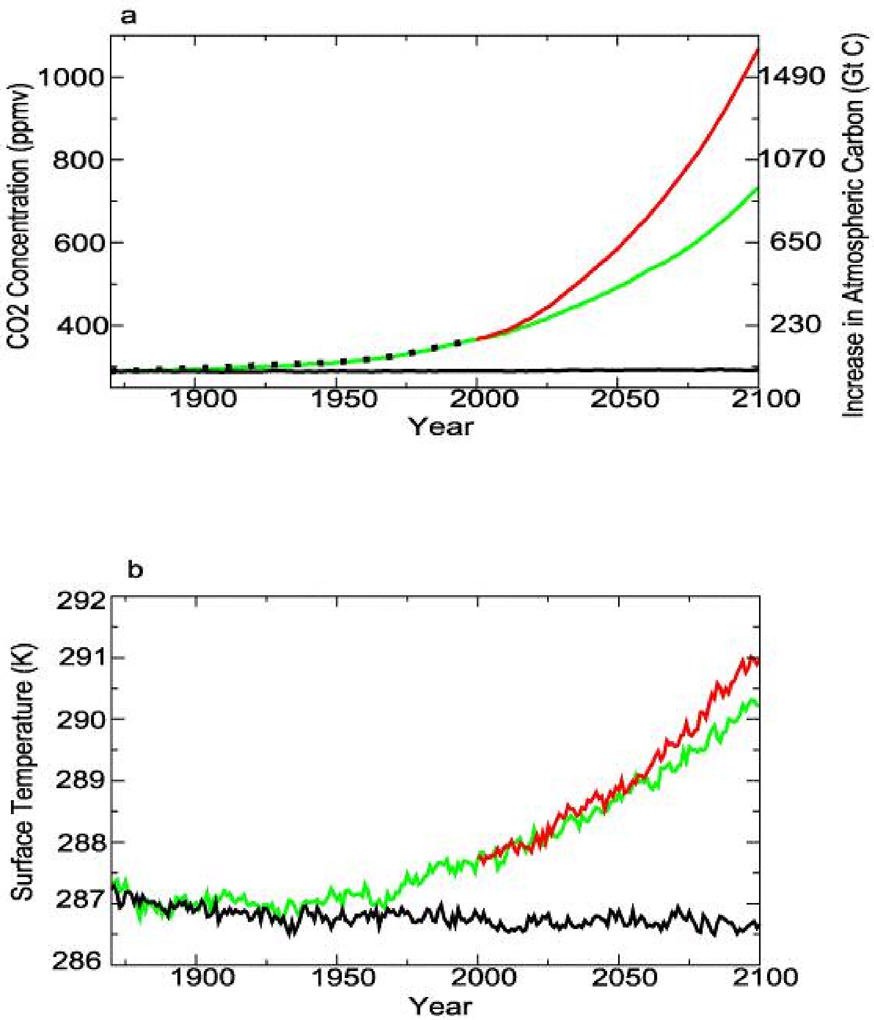

Section 2, Figure 2

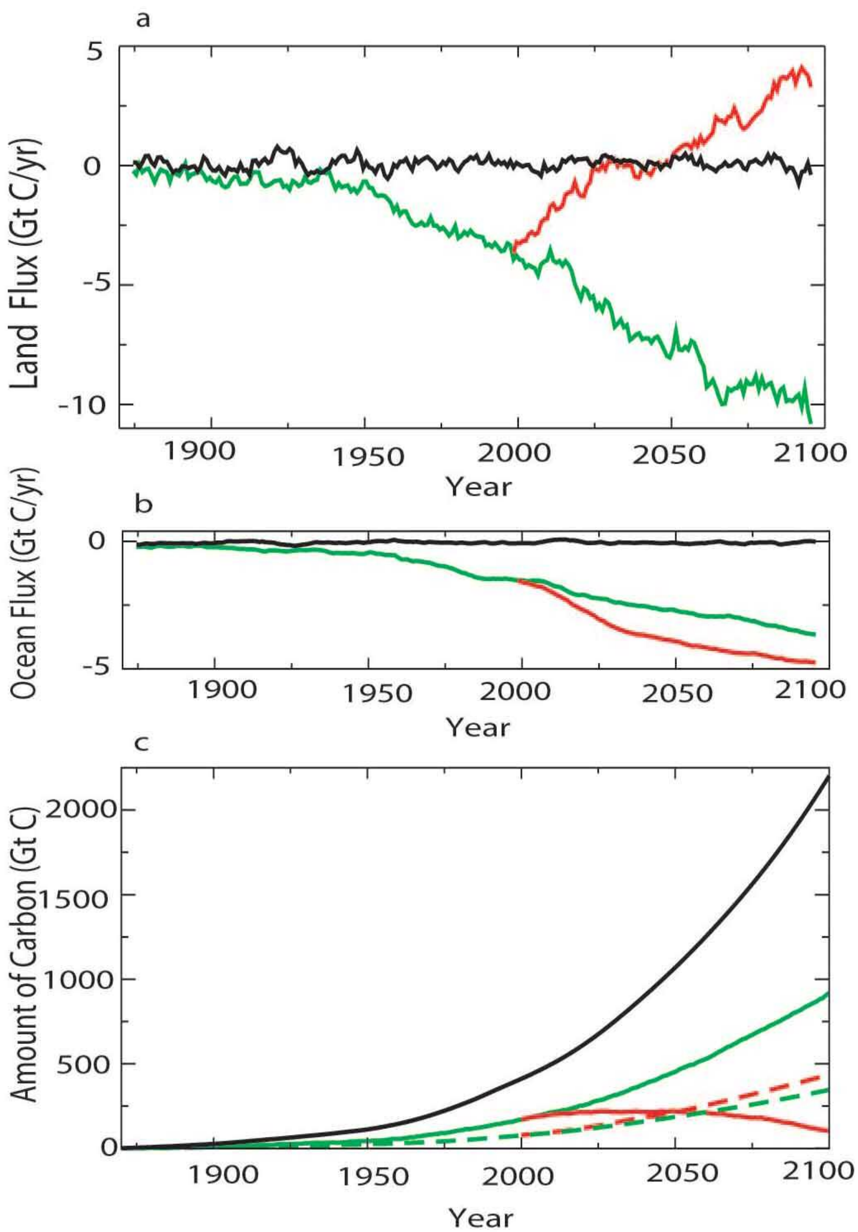

Section 2, Figure 3

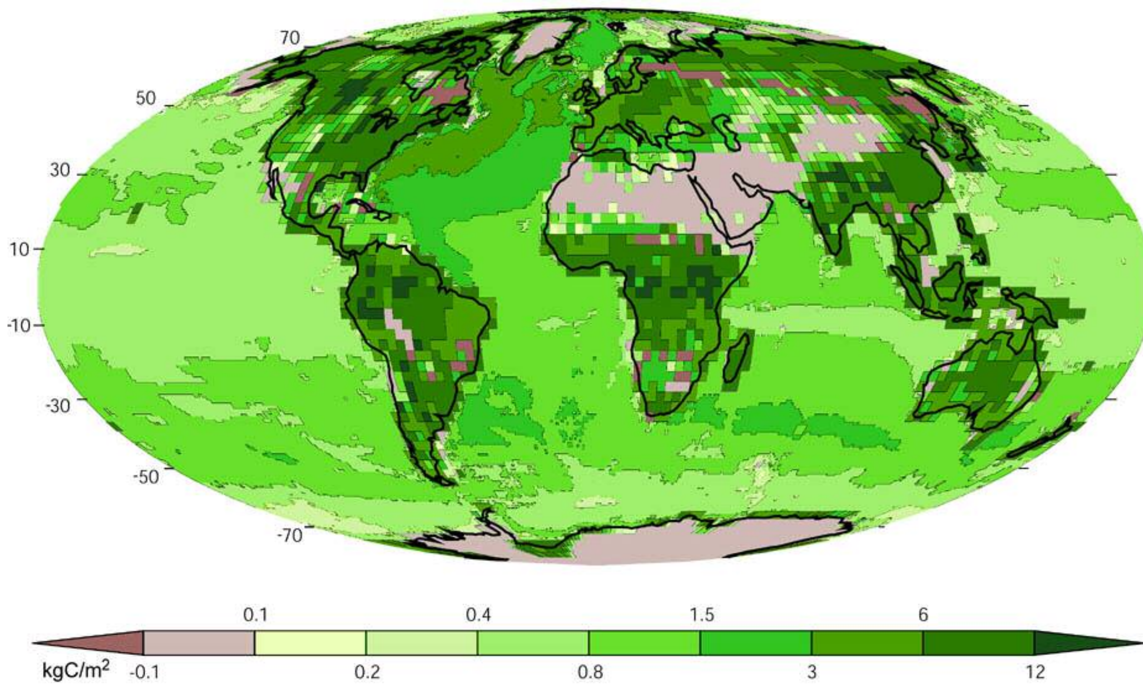

3. Dependence of carbon cycle feedback on climate sensitivity: Results from the INCCA coupled climate and carbon cycle model

Coupled climate and carbon cycle modeling studies have shown that the feedback between global warming and the carbon cycle, in particular the terrestrial carbon cycle, could accelerate climate change and result in larger warming. In this paper, we investigate the sensitivity of this feedback for year-2100 global warming in the range of 0 K to 8 K. Differing climate sensitivities to increased CO_2 content are imposed on the carbon cycle models for the same emissions. Emissions from the SRES A2 scenario are used. We use the LLNL INtegrated Climate and CArbon model, INCCA (i.e., the NCAR Parallel Coupled Model coupled to the IBIS terrestrial biosphere model and a modified-OCMIP ocean biogeochemistry model). In our model, for scenarios with year-2100 global warming increasing from 0 to 8 K, land uptake decreases from 47% to 29% of total CO_2 emissions. Due to competing effects, ocean uptake (16%) shows almost no change at all. Atmospheric CO_2 concentration increases were 48% higher in the run with 8 K climate change than in the zero-climate-sensitivity case. Our results indicate that carbon cycle amplification of climate warming will be greater if there is higher climate sensitivity to increased atmospheric CO_2 content**.**

The physical climate system and the global carbon cycle are tightly coupled, as changes in climate affect exchange of atmospheric CO_2 with theland surface and ocean . During the 1980s, oceanic and terrestrial uptake of carbon amounted to a quarter to a third of anthropogenic CO_2 emissions with strong interannual variability (Braswell et al., 1997; Prentice et al., 2000; 2001). Changes in these CO_2 fluxes affect Earth's radiative forcing and the physical climate system. A better understanding of carbon balance dynamics is required for interpreting variations in atmosphere-biosphere exchange (Fung et al., 1997) and for evaluating policies to mitigate anthropogenic CO_2 emissions (United Nations Framework Convention on Climate Change 1997; IGBP Terrestrial Carbon Working Group 1998).

Anthropogenic emissions of fossil fuels and land use change are expected to lead to significant climate change in the future (IPCC, 2001). Both climate change and elevated CO_2 have impact on land and ocean carbon uptake. Photosynthesis by plants will increase with increased atmospheric CO_2 content (the so-called CO_2 fertilization effect) because increased atmospheric CO_2 permits plant stomatal openings to narrow, thereby diminishing water loss and increasing water use efficiency. However, the enhanced physiological effects of CO_2 on productivity and water use efficiency asymptote at high CO_2 concentration (King et al., 1997; Cao and Woodward, 1998). Increased global temperatures are expected to increase heterotrophic respiration rates, diminishing or even reversing the CO_2 flux from the atmosphere to the land biosphere (Cox et al., 2000; Friedlingstein et al., 2001; Cramer et al., 2001; Joos et al., 2001). Studies on ocean carbon uptake have suggested that global warming reduces uptake of carbon by oceans (Sarmiento and Le Quere, 1996; Sarmiento et al., 1998). This occurs primarily because CO_2 is less soluble in warmer water and increased stratification would tend to inhibit downward transport of anthropogenic carbon.

One way to study the feedbacks between the physical climate system and carbon cycles is to use three-dimensional coupled ocean/atmosphere climate/carbon-cycle general circulation models. Two such models have published results representing the dynamical response of Earth's climate and carbon system to CO_2 emissions (Cox et al., 2000, Friedlingstein et al., 2001). The study by Cox et al. (2000) showed a very large positive feedback and the other study showed a much weaker feedback. A feedback analysis by Friedlingstein et al. (2003) indicated that the differences between the model results were due primarily to Southern Ocean circulation and land carbon response to global warming. However, land response to climate change was the dominant difference between the two model simulations of the 21st century. In the HadCM3 model (Cox et al., 2000), the land biosphere became a net source of CO_2 to the atmosphere, whereas in the IPSL model (Friedlingstein et al., 2001), the land biosphere was a net sink of CO_2 from the atmosphere.

Using the INtegrated Climate and CArbon (INCCA) model, we attempted in Section 2 of this report to bracket uncertainty in terrestrial uptake arising from uncertainty in the land-biosphere CO_2-fertilization effect. They performed one simulation in which the land-biosphere model was very sensitive to CO_2 fertilization and another simulation in which the land uptake was restrained by limiting CO_2 fertilization at present day levels. The fertilization-limited run was designed to represent the possibility that CO_2 fertilization effect could saturate rapidly, perhaps due to nutrient limitations. Through 2100 AD, the land was a very strong sink of carbon in the CO_2-fertilized simulation, but it became a source of carbon to the atmosphere in the fertilization-limited simulation. The predicted atmospheric CO_2 at year 2100 differed by 336 ppmv between the two cases. In the fertilization-limited run, the vegetation biomass was stable, but the soil carbon pool was shrinking because of climate change-induced increases in heterotrophic respiration.

The climate model used has a climate sensitivity (~ 2.1 K for a doubling of CO_2) near the low-end of the conventionally accepted range (1.5 to 4.5 K per CO_2-doubling; IPCC, 2001). The land surface is more likely to damp the effects of CO_2-emissions if climate sensitivity is low, with carbon uptake by the biosphere dominated by CO_2 fertilization. Higher climate sensitivity is more likely to amplify the effect of CO_2 emissions, because increased respiration rates at higher temperatures would be expected to induce carbon losses from the land biosphere. In this study, we address the dependence of terrestrial and ocean carbon uptakes on climate sensitivity using the coupled climate and carbon cycle model developed at LLNL. The major purpose is to investigate the sensitivity of carbon cycle feedbacks to climate sensitivity. The climate change range we have studied in this work is 0-8 K warming of global and annual mean surface temperature by 2100AD for the SRES A2 Scenario (IPCC, 2003). The warming produced here brackets the 1.4 – 5.8 K warming for year-2100 projected by IPCC (2001). Our results are from a single modeling study and validation using other coupled climate and carbon cycle models is required.

To investigate the sensitivity of the land and ocean carbon cycle to climate in the coupled climate system we use the INCCA (INtegrated Climate and CArbon) model of the dynamics and carbon-balance in the ocean, atmosphere, and land-surface. The physical ocean-atmosphere model is the NCAR PCM model (Washington et al., 2000), which is a version of the NCAR CCM 3.2 model (Kiehl et al., 1996) coupled to the LANL POP ocean model (Dukowicz and Smith, 1994; Maltrud et al., 1998). The climate model is coupled to a terrestrial biosphere model, Integrated Biosphere Simulator version 2 or IBIS2 (Foley et al., 1996; Kucharik, et. al., 2000) and an ocean biogeochemistry model. The horizontal resolution of land and atmosphere models is approximately 2.8° in latitude and 2.8° in longitude. The ocean model has a horizontal resolution of (2/3)°. The atmosphere and ocean models have 18 and 40 levels in the vertical, respectively.

Land surface biophysics, terrestrial carbon flux and global vegetation dynamics are represented in a single, physically consistent modeling framework within IBIS. IBIS simulates surface water, energy and carbon fluxes on hourly timesteps and integrates them over the year to estimate annual water and carbon balance. The annual carbon balance of vegetation is used to predict changes in the leaf area index and biomass for each of 12 plant functional types, which compete for light and water using different ecological strategies. IBIS also simulates carbon cycling through litter and soil organic matter. When driven by observed climatological datasets, the model's near-equilibrium runoff, Net Primary Productivity (NPP), and vegetation categories show a fair degree of agreement with observations (Foley et al., 1996; Kucharik, et. al., 2000).

The ocean biogeochemistry model is based on the Ocean Carbon-cycle Intercomparison Project (OCMIP) Biotic protocols (Najjar and Orr, 1999). This model predicts air-sea CO_2 fluxes, biogenic export of organic matter and calcium carbonate, and distributions of dissolved inorganic carbon, phosphate, oxygen, alkalinity, and dissolved organic matter. In the OCMIP protocol, export of biogenic materials is computed to maintain observed upper ocean nutrient concentrations. However, because our simulations involve changes in ocean circulation, we cannot make the assumption that surface nutrient concentrations remain stationary. Therefore, we replaced the OCMIP export formulation with a formulation based on that of Maier-Reimer (1993), as described in Section 2.

We developed a 1870 “pre-industrial” initial condition with more than 200 years of fully coupled equilibration before the start of experiments. During the first half of the spin up period, changes in soil carbon pools were accelerated by a factor of 40. We perform four model simulations starting from the pre-industrial initial conditions:

"Control” case with no change in forcing for the period 1870-2100. Climate drift evaluated for the period 1900-2100 is –0.35 K change in mean surface temperature (Table 1), about 6.4 % growth in sea ice extent, 14.2 % growth in ice volume, 3.14 ppmv increase in atmospheric CO_2 concentration, and 9.3 Gt C increase in soil carbon.

"1 x Sensitivity" case is the INCCA model in its standard configuration. The radiative forcing of atmospheric CO_2 on the climate system is calculated based on simulated atmospheric CO_2 content. CO_2 emissions are specified at historical levels for 1870-2000 (Marland et al., 2002) and SRES A2 levels from 2000-2100 (IPCC, 2001). Non-CO_2 greenhouse gas concentrations are specified at historical levels for 1870-2000 and SRES A2 levels from 2000-2100 (IPCC, 2001). Land use emissions are taken from Houghton (2003) for the historical period and from SRES A2 scenario thereafter. There is no change in aerosol forcing. In this scenario, total emissions reach 29 Gt-C per year in 2100 AD from present day values of 8 Gt-C per year.

"0 x Sensitivity" case is identical to the”1 x Sensitivity " case except that the radiation code continues to see the pre-industrial atmospheric CO_2 content, yielding a climate sensitivity of 0 K per CO_2-doubling. Though the land and ocean carbon cycle models are forced by the predicted atmospheric CO_2 concentration, the physical climate system is not. Our "0 x Sensitivity" case is similar to the uncoupled simulations in Cox et al. (2000) and Friedlingstein et al. (2001) except that our simulations are not performed offline.

"2 x Sensitivity" case is identical to the "1 x Sensitivity" case, except that the radiation code sees an amount of CO_2 in the atmosphere that would roughly double the radiative forcing from anthropogenic CO_2. The carbon cycle models use the actual predicted CO_2. Prescribed non-CO_2 greenhouse gas concentrations as seen by the climate system are also modified so that the radiative forcing is approximately twice that of "1 x Sensitivity". The methods used to modify the concentrations are as follows.

> The greenhouse gases used in our model are CO_2, CH_4, N_2O, CFC11 and CFC12. The functional dependence of radiative forcing on greenhouse gases is taken from IPCC (1997). Suppose we want N times the actual forcing. For CO_2, the forcing F is calculated as
>
> $F = K \ln (C(t)/Co)$,
>
> where C is the predicted concentration of CO_2 and Co is the pre-industrial concentration. K is a constant that varies with the model. We multiply C by the ratio$[C/Co]^{N-1}$ for performing the radiation calculations in the GCM to ensure approximately N times the actual forcing.
>
> Omitting the overlap terms, the radiative forcing for CH_4 and N_2O is given by $F = k (\mathrm{Sqrt}(M) - \mathrm{Sqrt}(Mo))$ where M is the concentration, Mo is the pre-industrial concentration, and k = 0.036 for CH_4 and k = 0.14 for N_2O. We multiply M by $[N + (1 - N)\ \mathrm{Sqrt}\ (Co/C)]^2$ to increase the radiative forcing by N times. Since the forcing of CFC11 and CFC12 varies linearly with their concentrations, we just multiply their concentrations by N to get N times the actual forcing.

This would be expected to roughly double the climate sensitivity of the model. We do not expect that the radiative forcing and climate change in 2 x Sensitivity will be exactly twice of that in 1 x Sensitivity for the following two reasons. First, we have used approximate formulae to double the forcings in 2 x Sensitivity. Secondly our results show that the predicted CO_2 concentration in 2 x Sensitivity is slightly higher than in 1 x Sensitivity.

The main purpose of these experiments is to provide a set of coupled climate/carbon-cycle simulations across which the only varying factor is climate sensitivity to increased atmospheric CO_2 concentrations. By keeping all other factors constant, we simplify analysis of our results.

The global and annual mean transient climate responses are listed in Table 1. The response is computed by differencing the averages for 2091-2100 AD and 1891-1900 AD. Since the climate drifts are small (Fig. 1), we do not subtract the drifts from these means. The evolution of global and annual means of surface temperature and atmospheric CO_2 concentration from the four simulations is shown in Fig. 1. The climate does not warm in the 0 x Sensitivity experiment, warms by about 3.2 K in the 1 x Sensitivity experiment, and by 8 K in the 2 x Sensitivity. Because our experiments are transient experiments, the change in net radiative flux at the top of the atmosphere in 1 x

Sensitivity and 2 x Sensitivity are not close to zero. The net imbalance in 2 x Sensitivity is 2.4 times that in 1 x Sensitivity. The warming in the 2 x Sensitivity run is 2.5 times that in 1 x Sensitivity, indicating that the climate response is approximately proportional to radiative forcing. Changes in other global variables such as precipitation, precipitable water and sea ice extent in 2 x Sensitivity are also more than twice the changes in the1 x Sensitivity run (Table 1). In the 2 x Sensitivity case, there is a decline of nearly 95 % of ice volume. We find that the sea ice disappears completely in both the hemispheres in their respective summers in that run.

The predicted CO_2 concentrations at 2100 in 1 x Sensitivity and 2 x Sensitivity are 732 and 857 ppmv respectively. Since the 2 x Sensitivity case has higher CO_2 concentrations, it actually has more than twice the CO_2 radiative forcing than in 1 x Sensitivity. This extra forcing of CO_2 in 2 x Sensitivity is about 2 Wm^{-2} and can explain nearly half of the extra 1.8 K warming. We neglected the negative overlap terms in the radiative forcing formulae for methane and nitrous oxide when we doubled the radiative forcing for these gases (Appendix A). Since these terms decrease the radiative forcing and we have neglected them, the 2 x Sensitivity case receives more than twice the radiative forcing of 1 x Sensitivity due to CH_4 and N_2O also.

The atmospheric CO_2 concentration increases from the pre-industrial level in the 0 x Sensitivity and 1x Sensitivity cases by 391 and 442 ppmv respectively (Fig. 1). The difference is only 51 ppmv between the 0 x Sensitivity and 1 x Sensitivity cases. Cox et al. (2000) and Friedlingstein et al. (2001) obtained differences of about 250 and 100 ppmv respectively in their models. Their year-2100 warmings were 5.5 and 3 K respectively. The "carbon cycle feedback factor" is defined as the ratio of CO_2 change when climate is changing to the CO_2 change when climate is constant (Friedlingstein et al., 2003). The implied net carbon cycle feedback factor in our simulations is 1.13. The net carbon cycle feedback factors are 1.19 and 1.675 in Friedlingstein et al. (2001) and Cox et al. (2000) respectively. Therefore, our model shows the weakest feedback between climate and carbon cycle among the existing coupled climate and carbon cycle models. However, the CO_2 in the 2 xSensitivity case increases by 578 ppmv and the carbon cycle feedback factor increases to 1.48. Atmospheric CO_2 concentrations are 176 ppmv higher in the run with 8 K climate change than in the run with no climate change. Therefore, there is a nonlinear increase in the carbon cycle feedback with warming.

The global and annual mean net land and ocean uptakes are shown in Fig.2. The interannual variability is smoothed by performing a 5-yr running mean. The land uptake increases monotonically with time in the 0 xSensitivity case and it reaches values larger than 10 Gt-C per year by 2100 AD, more than a third of the emission rate at that time. The effect of CO_2 fertilization is probably exaggerated in these simulations because we do not consider factors other than limitation by sunlight, water, and carbon dioxide. Inclusion of other factors, such as nitrogen or phosphate limitation might diminish the magnitude of the response to added CO_2 (Hungate et al. 2003). Compared to similar models, IBIS also tends to simulate higher fertilization effect (Mc Guire et al, 2001). Land uptake of carbon is similar in the 0 x Sensitivity and 1x Sensitivity cases up to 2070 AD; after this the 1 x Sensitivity case takes up less carbon than the 0 x Sensitivity case because of increase in heterotrophic (soil microbial) respiration (Fig.3). The larger warming in 2 x Sensitivity results in significantly increased soil microbial respiration and reduced land uptake of carbon (Fig.3); soil carbon content declines after 2050. The land biosphere takes up less than half the carbon it takes up in the 0 x Sensitivity case after 2050 (Fig.2). Interannual variability increases in all cases after 2050, presumably because of the larger carbon pools in the terrestrial biosphere.

Our results are in agreement with Friedlingstein et al. (2001) who obtained reduced land uptake with climate change in the IPSL model when CO_2 concentrations were increasing at 1% per annum. However, our results are in sharp contrast to Cox et al. (2000) who showed that land becomes a source of carbon around 2050 AD when they forced their model HadCM3 with IS92a scenario. With the HadCM3 model, a drying and warming of the Amazon initiates a collapse of the tropical forest followed by large releases of soil carbon. Such a loss of vegetation biomass and soil carbon content does not occur in our 1 x Sensitivity simulation (Fig. 3). The increase of global mean Net Primary Productivity (NPP) with time is very similar in the 0 x, 1 x, and 2 x Sensitivity experiments. We do not see any sign of declines in biomass with warming even in the 2 x Sensitivity case. In 1 x Sensitivity, both vegetation biomass and soil carbon are increasing since the warming is only 3.2 K (as opposed to 5.5 K in HadCM3). In 2 x Sensitivity, soil carbon is decreasing because of increased respiration due to a 8 K warming, but biomass still keeps increasing (Fig. 3).

For the 0 x Sensitivity run, ocean uptake also shows a monotonic increase in uptake up to 2100 AD because of rising atmospheric CO_2 (Fig.2). The uptake reaches about 3.5 Gŧ C per year, only a third of the land uptake. This may be an underestimate, as the model tends to underestimate historical ocean carbon uptake (see Section 2). Ocean uptakes in 1 x Sensitivity and 2 x Sensitivity are similar to the 0 x Sensitivity run. Apparently, the increase in uptake due to further increases in atmospheric CO_2 in these simulations is offset by the decrease in uptake due to warming. Surface warming tends to reduce the dissolution of atmospheric CO_2 in the ocean. Surface warming also causes increased thermal stratification, which inhibits downward transport of anthropogenic carbon. However, with increased stratification, the residence time of nutrients in the euphotic zone increases, allowing a greater fraction of nutrients to be exported from the surface layers as particulate organic carbon. This effect tends to counteract some of the direct physical effects of increased stratification (Sarmiento et al., 1998).

In HadCM3 and IPSL simulations, climate change in their “1 x Sensitivity” simulations produced lessoce an carbon uptake than in their “0 x Sensitivity” simulations (Cox et al., 2000; Friedlingstein et al., 2003). Our ocean model results are more similar to those of Cox et al. (2000; uptake in HadCM3 was ~ 5 Gt-C per year) than those of Friedlingstein et al (2001). In the IPSL simulation (Friedlingstein et al., 2001), ocean uptake was ~ 10 Gt-C per year in the “0 x Sensitivity” simulation due to strong convection in the Southern Ocean; this uptake decreased moderately in their “1 x Sensitivity” simulation.

Under the SRES A2 scenario, total emissions reach 29 Gt-C per year at year 2100 AD. Cumulative anthropogenic emissions for the period 1870 to 2100 amounts to 2200 Gŧ C. The amounts taken up by land and ocean are shown in Fig.4. In the 0 x Sensitivity case, land takes up 1031 Gt-C, nearly 50 percent of the emissions (Fig. 4a). The uptake is reduced to 919 and 629 Gt-C in 1 x Sensitivity and 2 x Sensitivity runs respectively. Therefore, land uptake decreases from 47 to 29 % (1031 to 629 Gŧ C) of the total emissions as the global temperature change increases from 0 to 8 K in our model. HadCM3 modeling study showed a range of –5 to 34 % (–100 Gŧ C to 650 Gt-C) of the

1900 Gt-C emissions of the IS92a scenario for the same temperature range (Cox et al., 2000; Friedlingstein et al., 2003). Therefore, there is a large range of model projections of future land uptake in current coupled climate/carbon models. Friedlingstein et al. (2003) demonstrated that the climate impact on the land carbon cycle is mainly responsible for the large difference in the overall response of the IPSL and HadCM3 models.

Total ocean uptake in our 0 x Sensitivity, 1 x Sensitivity and 2 x Sensitivity cases differ little (Fig. 4b). The net uptake over the period 1870-2100 is around 350 Gt-C in all the runs. Therefore, future ocean carbon uptake appears to be relatively insensitive to uncertainty in climate sensitivity in our model for specified CO_2 emission scenarios. In agreement with our results, Cox et al. (2000) and Fridlingstein et al. (2001) obtained only modest sensitivity of the ocean carbon uptake to climate change in HadCM2 and IPSL models.

The fraction of the cumulative anthropogenic emissions that remains in the atmosphere at any time since 1870 depends on the climate change (Fig. 4c). Since the averaging time interval increases with time, the fractions exhibit little variability in the later periods and the curves become smooth towards the end of simulations. The fractions from all the runs are close to each other until 1970. After that, they diverge from each other. In 0 x Sensitivity, only 37% of the total emissions remain in the atmosphere by 2100 AD. This fraction reaches 43% and 55% in 1 x Sensitivity and 2 x Sensitivity respectively. Therefore, the fraction of emissions that remains in the atmosphere increases with warming primarily because the land uptake declines with warming.

IBIS simulates the present day distribution of vegetation quite realistically (Foley et al., 1996) when forced with the observed climate. Dominantvegetation distribution s from our simulations for the period 2071-2100 are shown in Fig. 5. We use kappa statistics (Monserud, 1990) to compare maps of vegetation distributions. Kappa takes on a value of 1 with perfect agreement. It has a value close to zero when the agreement is approximately the same as would be expected by chance. A kappa value of 0.47 (fair agreement; Landis and Koch, 1977) is obtained for a comparison of IBIS simulated vegetation and observations (Foley et al., 1996).

Global comparison of control vegetation distributions with distributions from 0 x, 1 x, and 2 x Sensitivity runs give kappa values of 0.80 (very good agreement), 0.54 (good) and 0.40 (fair) respectively. The high kappa value for comparison between control and 0 x Sensitivity suggest that atmospheric CO_2 changes have weaker influence on changing the vegetation distribution than climate change; 0 x Sensitivity run has no climate change but it has carbon cycle changes due to fossil fuel emissions. However, as the global warming increases, vegetation distribution changes dramatically; kappa value decreases from 0.8 to 0.4 when the warming increases from 0 to 8 K.

In terms of area occupied by different vegetation types, tropical and temperate forests expand significantly with global warming (Fig.5; Table 2). The area covered by them increases from about 40 % in the control case to nearly 60 % of the land area in 2 x Sensitivity. In general there is a migration of tropical, temperate, and boreal forests poleward with warming, leading to significant declines in area occupied by tundra and polar deserts (land ice) in the 2 x Sensitivity run. We caution that climate change and CO_2 fertilization could also impact ecosystem goods and services not represented by our terrestrial ecosystem model, such as species abundance and competition, habitat loss, biodiversity and other disturbances (Root and Schneider, 1993).

In this paper, we investigate the sensitivity of the positive feedback between climate change and carbon cycle for a range of climate sensitivities to increased atmospheric CO_2 content; nominally, 0, 2 and 4 K per doubling of atmospheric CO_2 content. With the SRES A2 emission scenarios, this produces a simulated year-2100 global warming ranging from 0 K to 8 K. We found that the land biosphere takes up less carbon with higher climate sensitivity, and this is not compensated for by increased ocean carbon uptake. Thus, the higher climate sensitivity simulations are warmer both because of increased sensitivity to added CO_2, but also because more CO_2 remained in the atmosphere.

In our model, cumulative land uptake varies between about 29 and 47 % of the total emissions for a 0-8 K range in temperature change. Ocean uptake (16%) shows almost no change at all. The fraction of the total emissions that remains in the atmosphere ranges from 37 to 55% under different climate changes. Atmospheric CO_2 concentrations are 176 ppmv higher in the run with 8 K climate change than in the no climate change run. Our results are in agreement with other modeling studies that concluded that the climate impact of land carbon cycle is mainly responsible for the modeling uncertainty in the projection of future atmospheric CO_2 concentrations.

In sharp contrast to Cox et al. (2000) but in agreement with Friedlingstein et al. (2001), our land carbon cycle model does not become a net source of carbon to the atmosphere even when the warming is as high as 8K. In HadCM3 (Cox et al., 2000), vegetation carbon in Amazon begins to decline, as a drying and warming of Amazonia initiates loss of forest. Such a loss of vegetation biomass does not occur in our simulations. In our model, soil carbon does show declines by 2100 AD for an 8 K global warming. This results in reduced land uptake of carbon. However, the vegetation biomass keeps increasing. The effect of CO_2 fertilization is probably exaggerated in our simulations because we do not consider factors other than limitation by sunlight, water, and carbon dioxide.

In Section 2 we bracketed the uncertainty in land uptake due to CO_2 fertilization. Here we have shown how land fluxes may depend on climate sensitivity to CO_2 itself In Section 2 we showed that atmospheric CO_2 concentrations are 336 ppmv higher in the fully fertilized case than the fertilization-capped case, a sensitivity about twice we find for a 0-8 K range in global warming.

The high sensitivity of our terrestrial biosphere model to CO_2 may be associated with the lack of nutrient cycles (e.g., nitrogen, phosphorous, etc.). In the real world, as opposed to our model, CO_2-fertilized ecosystems may run into nutrient limitations. Changes in nitrogen availability are important to the carbon cycle through changes in plant nutrient availability (Schimel, 1998; Nadelhoffer et al., 1999; Hungate et al., 2003). Models that include nitrogen limitation show less sensitivity of CO_2 fluxes for changes in atmospheric CO_2 (Cramer et al., 2001).

Whether the land-biosphere damps or amplifies global warming seems to depend on highly uncertain assumptions regarding the response of the biosphere to increased CO_2 and a changed climate. These uncertainties could perhaps be narrowed with investigation of carbon dynamics across a broad range of ecosystems and climate regimes, often including manipulation experiments, and redoubled efforts to represent those dynamics numerically.

Section 3, References

Cao, M., and F. I. Woodward, Dynamic responses of terrestrial ecosystem carbon cycling to global climate change, *Nature*, **393**, 249-252, 1998.

Cramer, W., A. Bondeau, F. I. Woodward, et al., Global response of terrestrial ecosystem and funtion to CO2 and climate change: results from six dynamic global vegetation models, *Global Change Biology*, **7**, 357-373, 2001.

Cox, P. M., R. A. Betts, C. D. Jones, S. A. Spall, and I. J. Totterdell, Acceleration of global warming due to carbon-cycle feedbacks in a coupled model, *Nature*, **408**, 184-187, 2000.

Dukowicz, J. K., and R. D. Smith, Implicit free-surface method for the Bryan-Cox_Semtner ocean model, *J. Geophys. Res*., **99**, 7991-8014, 1994.

Foley, J. A., I. C. Prentice, N. Ramankutty, S. Levis, D. Pollard, S. Sitch, A. Haxeltine, An integrated biosphere model of land surface processes, terrestrial carbon balance and vegetation dynamics, *Global Biogeochem. Cycles*, **10**, 603-628, 1996.

Friedlingstein, P., L. Bopp, P. Clais, et al., Positive feedback between future climate change and the carbon cycle, Geophys. Res. Lett., 28, 1543-1546, 2001.

Friedlingstein, P., J.-L. Dufresne, P. M. Cox, and P. Rayner, How positive is the feedback between climate change and the carbon cycle? *Tellus*, **55B**, 692-700, 2003.

Fung, I., C. B. Field, J. A. Berry, et al., Carbon 13 exchanges between the atmosphere and biosphere, *Global Biogeochemical Cycles*, **11**, 507-533, 1997.

Houghton, R., Revised estimates of the annual net flux of carbon to the atmosphere from changes in land use and land management 1850-2000, *Tellus*, **55B**, 378-390, 2003.

Hungate, B. A., J. S. Dukes, M. R. Shaw, Y. Luo, and C. B. Field, Nitrogen and Climate Change, *Science*, **302**, 1512-1513, 2003.

Intergovernmental Panel on Climate Change (IPCC), An introduction to simple climate models used in the IPCC second assessment report, IPCC Technical paper II, J. T. Houghton, L. G. M. Filho, D. J. Griggs and K. Masket (eds.), 1997.

Intergovernmental Panel on Climate Change (IPCC), *Climate Change 2001*, *The Scientific Basis*, Cambridge University Press, New York, USA, 2001.

Joos, F., I. C. Prentice, S. Sitch, et al., Global warming feedbacks on terrestrial carbon uptake under the Intergovernmental Panel on Climate Change (IPCC) emission scenarios, Global Biogeochemical Cycles, 15, 891-907, 2001.

Kiehl, J. T., J.J.Hack, G.B.Bonan, B.Y.Boville, B.P.Briegleb, D.L.Williamson, and P.J.Rasch, Description of the NCAR Community climate Model (CCM3). *NCAR Tech. Note*. NCAR/TN-420+STR, 1996.

King, A. W., W. M. Post, and S. D. Wullschleger, The potential response of terrestrial carbon storage to changes in climate and atmospheric CO2, *Climate Change*, **35**, 199-227, 1997.

Kucharik, C. J., et. al., Testing the performance of a dynamic global ecosystem model: Water balance, carbon balance, and vegetation structure, *Global Biogeochem. Cycles* **14** (3), 795 (2000).

Landis, J. R., and G. G. Koch, The measurement of observer agreement for categorical date, *Biometrics*, **33**, 159-174, 1977.

Maier-Reimer, E., 1993. Bigeochemical cycles in an ocean general-circulation model — Preindustrial tracer distributions, *Global Biogeochemical Cycles* **7(3)**: 645-377.

Monsrrud, R. A., Methods for comparing global vegetation maps, IIASA *WP-90-40*, Int. Inst. For Appl. Syst. Anal., Laxenburg, Austria, 1990.

Maltrud, M. E., R. D. Smith, A. J. Semtner, and A. J. Malone, Global eddy-resolving ocean simulations driven by 1985-1995 atmospheric winds, *J. Geophys. Res*., **103**, 30825-30853, 1998.

Marland G, T. Boden, and R. Andres, Global, regional, and national annual CO2 emissions from fossil-fuel burning, cement production and gas flaring: 1751-1999, *CDIAC NDP-030*, Carbon Dioxide Information Analysis Center, Oak Ridge National Laboratory, Tennessee.

McGuire, A.D., S. Sitch, J.S. Clein, R. Dargaville, G. Esser, J. Foley, M. Heimann, F. Joos, J. Kaplan, D.W. Kicklighter, R.A. Meier, J.M. Melillo, B. Moore III, I.C. Prentice, N. Ramankutty, T. Reichenau, A. Schloss, H. Tian, L.J. Williams, and U. Wittenberg (2001). Carbon balance of the terrestrial biosphere in the twentieth century: Analyses of CO2, climate and land-use effects with four process-based ecosystem models. *Global Biogeochemical Cycles*, **15**, 183-206, 2001.

Nadelhoffer, K. J., B. A. Emmett, P. Gundersen, et al., Nitrogen makes a minor contribution to carbon sequestration in temperate forests, *Nature*, **398**, 145-148, 1999.

Najjar, R.G., and J.C. Orr, 1999, Biotic How-To, Revision 1.7, Ocean Carbon-cycle Model Intercomparison Project (OCMIP), thttp://www.ipsl.jussieu.fr/OCMIP/phase2/simulations/Biotic/HOWTO-Biotic.html

Prentice, I. C., M. Heimann, S. Sitch, The carbon balance of the terrestrial biosphere; ecosystem models and atmospheric observations, *Ecological Applications*, **10** (6), 1553-1573, 2000.

Prentice, I. C., *et al. Climate Change 2001: The Scientific Basis: Contribution of Working Group I to the Third Assessment Report of the IPCC*, J.T. Houghton *et al.*, Eds. Cambridge University Press, UK, pp. 183–237 (2001).

Root, T.L. and S. H. Schneider, Can large scale climatic models be linked with multiscale ecological studies?, *Conservation Biology*, **7**, No.2, 256-270, 1993.

Sarmiento, J.L., and C. Le Quere, Oceanic carbon dioxide uptake in a model of century-scale global warming, *Science*, **274**, 1346-1350, 1996.

Sarmiento, J. L., and M. C. Hughes, R. J. Stouffer and S. Manabe, Simulated response of the ocean carbon cycle to anthropogenic climate warming, *Nature*, **393**, 245-249, 1998.

Schimel, D. S., The Carbon equation, *Nature*, **393**, 208-209, 1998.

Washington, W. M., J. W. Weatherly and others, Parallel Climate Model (PCM) control and transient simulations, *Climate Dynamics*, **16**, 755-774, 2000.

Table 1. Changes in Global and annual mean model results (decade of 2091-2100 minus 1891-1900)

Experiment	Surface Temp. (K)	Precip. (%)	Water vapor (kgm^{-2}) (%)	Sea ice extent (%)	Sea ice volume (%)	Net flux at TOA (Wm^{-2})
Control	-0.35	-0.52	-0.28 (-1.3)	6.4	14.2	0.14
0 x Sensitivity	-0.03	-0.03	-0.17 (-0.8)	3.7	0.9	0.03
1 x Sensitivity	3.17	5.03	4.87 (22.9)	-26.0	-66.0	1.56
2 x Sensitivity	8.00	11.63	13.71 (64.2)	-79.1	-94.5	3.77

Table 2. Fraction of land area occupied by vegetation types during 2071-2100

Vegetation type	Control	0 x Sensitivity	1 x Sensitivity	2 x Sensitivity
Tropical forests	22.2	24.2	24.6	30.3
Temperate forests	19.3	22.7	24.3	29.0
Boreal forests	6.7	8.2	10.6	5.8
Savanna, Grasslands & Shrublands	12.5	8.5	11.8	12.9
Tundra	6.9	8.8	6.5	2.6
Desert	16.4	14.5	12.3	13.4
Polar desert	16.0	13.1	7.9	6.0

Section 3, Figure Captions

Figure 1 Evolution of global and annual mean surface temperature (upper panel) and atmospheric CO_2 concentration (lower panel). Atmospheric CO_2 concentrations are 51 (176) ppmv higher in the 1 x Sensitivity (2 x Sensitivity) run with 8 K climate change than in the 0 x Sensitivity run with no climate change.

Figure 2 Evolution of the 5-yr running mean of global, annual flux of carbon from land to atmosphere (upper panel) and from ocean to atmosphere (lower panel). Negative values represent fluxes into land and ocean. Land fluxes are reduced to half when the climate change is doubled and ocean fluxes are insensitive to climate change in our model.

Figure 3 Evolution of Net Primary Productivity (NPP) and heterotrophic (soil microbial) respiration (upper panel) and changes in vegetation biomass and soil carbon content (lower panel). The increase in biomass is similar in 0 x, 1 x, and 2 x Sensitivity experiments because the NPPs are similar. Soil carbon change in 1 x Sensitivity is smaller that 0 x Sensitivity because of increase in soil microbial respiration. Further increases in soil respiration in 2 x Sensitivity leads to declines in soil carbon content after 2050.

Figure 4 Evolution of cumulative carbon uptakes by land (upper panel) and oceans (middle panel) since the pre-industrial period. The air-borne fraction of cumulative emissions is shown in the bottom panel. Our results suggest a large range in land uptake, and air-borne fraction, and little change in ocean uptake over the 0-8 K range of global warming.

Figure 5 Vegetation distributions in our simulations. Antarctica is not shown. The area covered by tropical and temperate forests increases dramatically when global warming increases from 0 to 8 K. There is a also migration of tropical, temperate, and boreal forests poleward with warming, leading to significant declines in area occupied by tundra and polar deserts (land ice) in the 2 x Sensitivity run.

Section 3, Figure 1

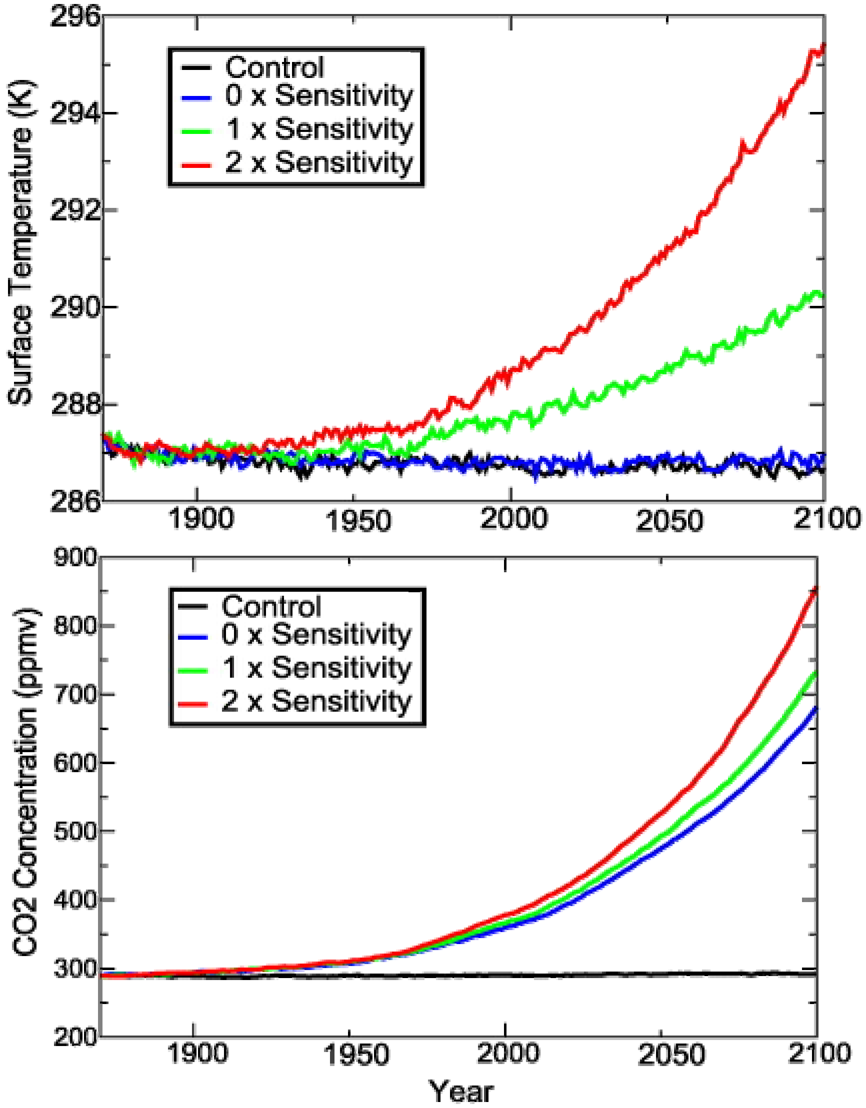

Section 3, Figure 2

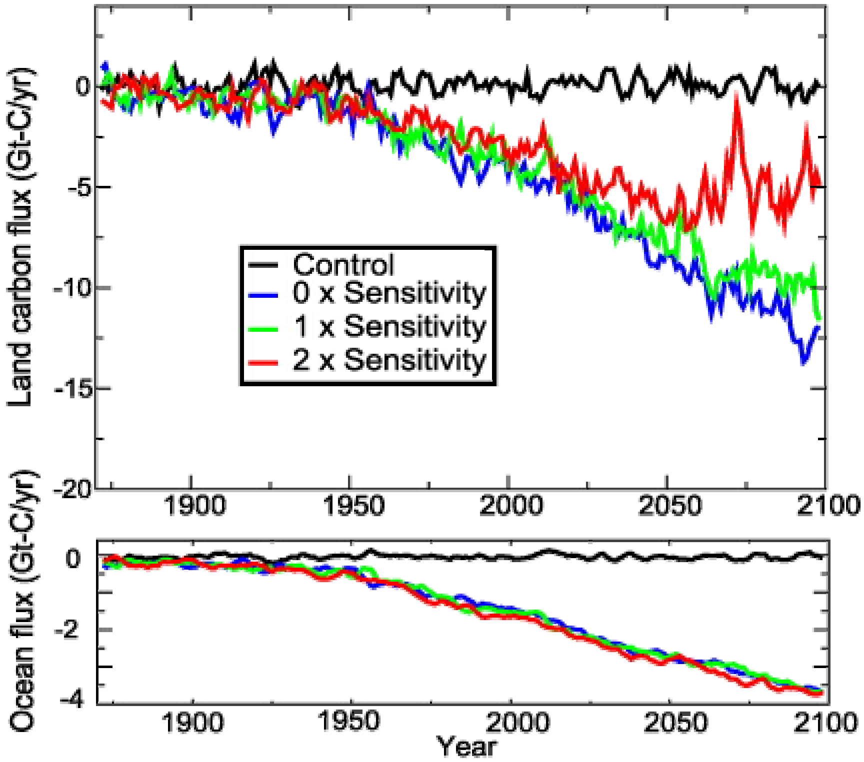

Section 3, Figure 3

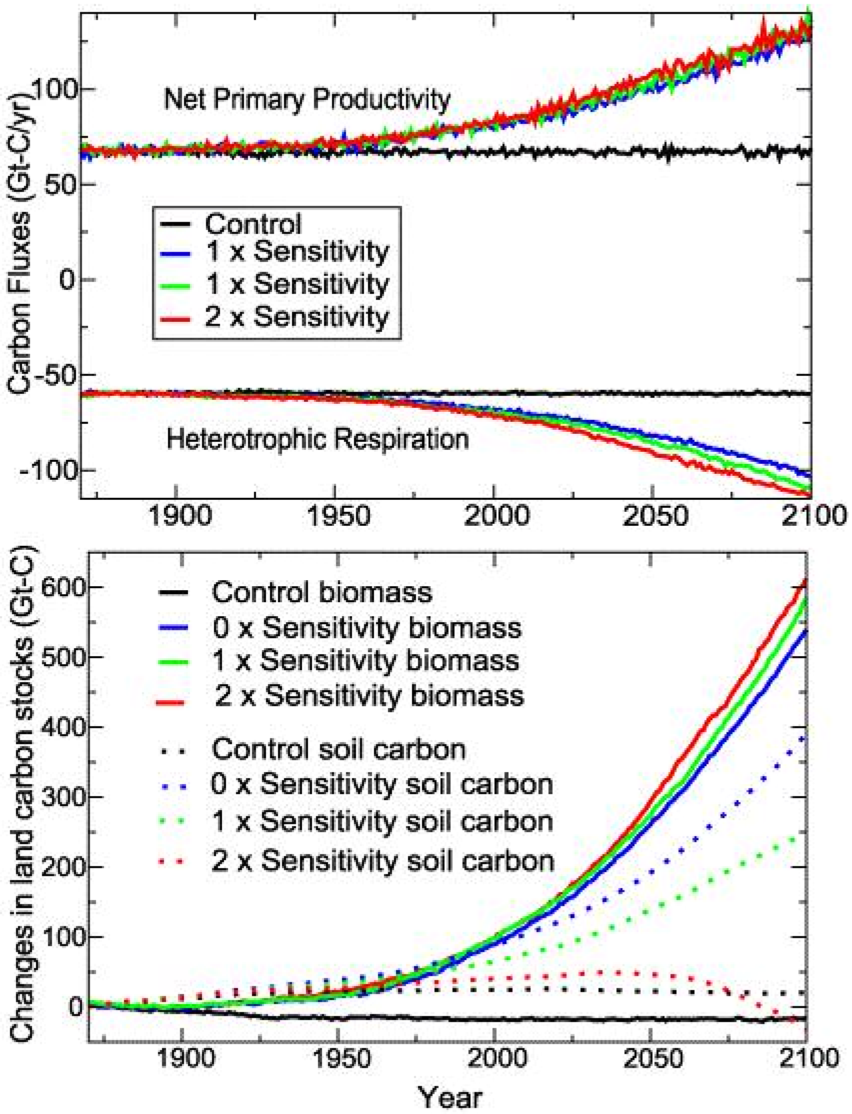

Section 3, Figure 4

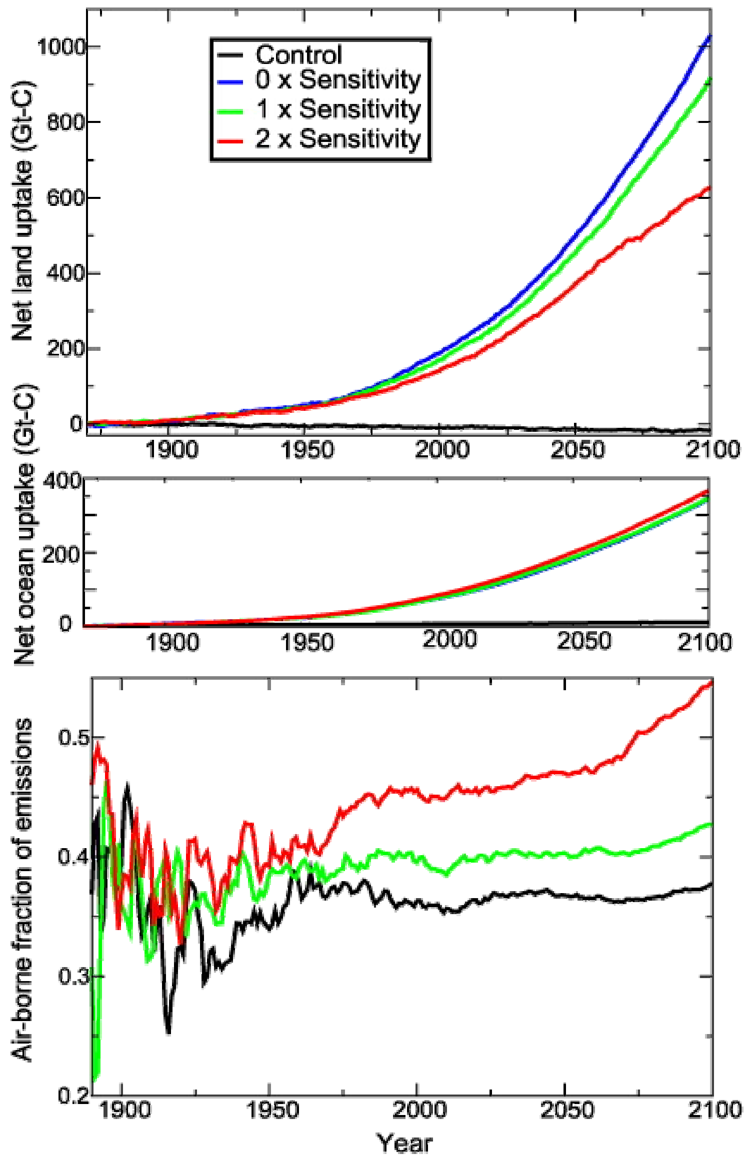

Section 3, Figure 5